Electric-Field-Induced Chirality in Columnar Liquid Crystals

Alberto Concellón, Ru-Qiang Lu, Kosuke Yoshinaga, Hsiu-Fu Hsu, and Timothy M. Swager*

*Department of Chemistry, Massachusetts Institute of Technology, 77 Massachusetts Avenue, Cambridge, Massachusetts 02139, United States. * Email: tswager@mit.edu*

ABSTRACT: We describe a novel class of tetraphenylbenzene-based discotic molecules with exceptional self-assembling properties. Absorption and fluorescence studies confirmed the formation of *J*-type aggregates in solution. The discotic mesogens also show an enhancement of the emission upon aggregation. Interestingly, these discotic molecules displayed enantiotropic hexagonal columnar liquid crystal phases that can be switched into a helical columnar organization by application of an electric field. The helical columns arise from the electric-field-induced tilt of the polar fluorobenzene ring that directs all of peripheral phenyl groups into a propeller-like conformation with respect to the central benzene core. A cooperative assembly process of these propeller-shaped molecules resolves into a helical columnar organization, in which the preferred helical sense is obtained from the stereogenic center proximate to the polar carbon-fluorine bond. The ease of inducing chirality in columnar LCs by electric field presents opportunities to create next-generation chiral materials for a variety of applications.

INTRODUCTION

Nature makes use of complex helical structures (e.g. protein α-helix, DNA double helix) in recognition, replication and selective activity.[1-2] Mimicking these biological systems has inspired materials chemists to pursue a wide range of artificial helical molecules, polymers, and self-assembled small molecule aggregates.[3-6] Synthetic helical architectures have demonstrated unique chiral phenomena, and specific functionalities, which have not been observed in natural systems.[7] Liquid crystals (LCs) are one of the most appealing synthetic systems and chirality is transferred from molecular to much longer length scales.[8-10] The unique combination of long-range order and fluidity with chirality has resulted in LC phases with unprecedented structures and properties.[11-12] Among chiral LCs, columnar phases represent a powerful tool to achieve helical columnar assemblies that can further promote two-dimensional arrangements.[13] Helical intracolumnar order often lies on the formation of twisted assemblies as a result of the steric interactions between adjacent cores that leads to a rotational offset.[14] Additionally, molecular chirality of stereogenic centers located in the flexible alkyl chains at the periphery of the disk-like cores can be transferred to the supramolecular organization and guide the packing direction. In cases with propeller types of structures the small chiral biases have been observed to promote cooperative helical columnar phases.[15] Exotic helical superstructures have proven interesting, and several research groups have recently demonstrated unusual electro-optical behavior, chiro-optical properties, ferroelectricity, or exceptional non-linear optical properties.[16-21]

Herein, we report on the exceptional self-assembling features of discotic molecules based on a tetraphenylbenzene core (**Figure 1**). Discotic molecule **3** was designed to incorporate a chiral alkyl chain as well as a carbon-fluorine bond conformationally coupled to the chiral center, whereas **1** was designed to have an achiral structure for comparison purposes. The lateral fluoro substituent was introduced into the discotic molecule to generate a strong dipole moment, and hence electric field response.[22-23] These discotic molecules displayed enantiotropic columnar liquid crystal phases over a wide temperature range. Such columns are formed from discotic molecules which are conformationally dynamic and are essentially free to rotate around their short optical axis, thereby resulting in an achiral columnar phase. We hypothesized that the dihedral angle of the C−C bond connecting the fluorobenzene ring and the central benzene could be biased with an external electric field to produce a propeller-like configuration. The propeller shape, and the transference of chirality from the stereogenic center proximate to the fluorine, creates an excess of an enantiomeric conformer and mesogens efficient pack in a helical columnar organization (**Figure 1**).

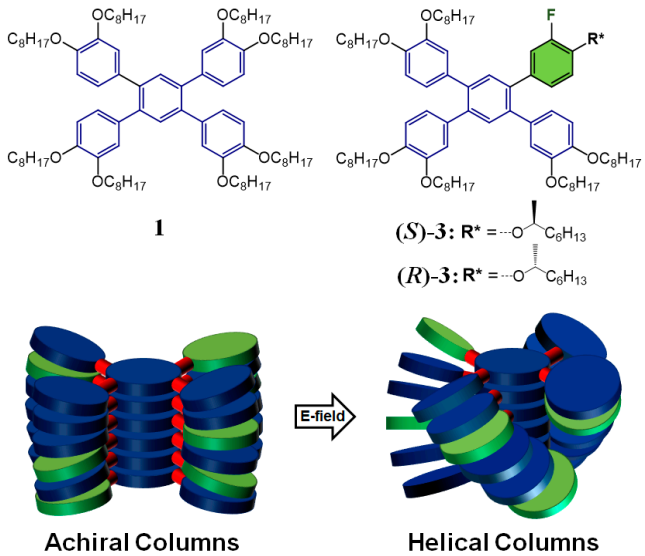

Figure 1. Chemical structure of the electric-field switchable discotic liquid crystals, and schematic representation of its self-assembly into (helical) columns.

RESULTS AND DISCUSSION

The aryl boronic acids were prepared following previously reported procedures.[24-25] **1** was synthesized in 95% yield by a 4-fold Suzuki coupling reaction of 1,4-dibromo-2,5-diiodobenzene with 3,4-bis(octyloxy)phenylboronic acid (**Scheme 1**). Synthesis of compound **3** began with the mono-coupling reaction of 1,4-dibromo-2,5-diiodobenzene with (*S*)- or (*R*)-(3-fluoro-4-(octan-2-yloxy)phenyl)boronic acid to afford **2** in 40-47% yield. Functionalization of the remaining halide groups of **2** was accomplished using excess of 3,4-bis(octyloxy)phenylboronic acid to produce **3** in 77-84% yield. All compounds were purified by column chromatography and isolated as air-stable waxy solids, which are soluble in common organic solvents (dichloromethane, chloroform, ethyl acetate or tetrahydrofuran). ^{1}H and ^{13}C NMR spectra of **1** and **3** are consistent with the proposed chemical structures, and mass spectrometric analysis showed the expected *m/z* peak (**Figures S1-S6**). Moreover, we observed a concentration-dependent behavior of ^{1}H NMR spectra, wherein an upfield shifting was detected for all aromatic proton signals upon increasing concentration (**Figure 2**). This effect is the result of mutual shielding from the close proximity between aromatic rings, and reveals that **1** and **3** tend to self-assemble in solution *via* π–π stacking. It is noteworthy that the protons of the central benzene core (H_A) experienced the largest shift in the ^{1}H NMR spectra. The observed changes in chemical shift suggests a preferred conformation in which each discotic molecule is rotated with respect to the next molecular unit. This twisting in the stacking places the affected protons in the cone-shaped shielding zone of the aromatic system, explaining their strong shifting.[26-27]

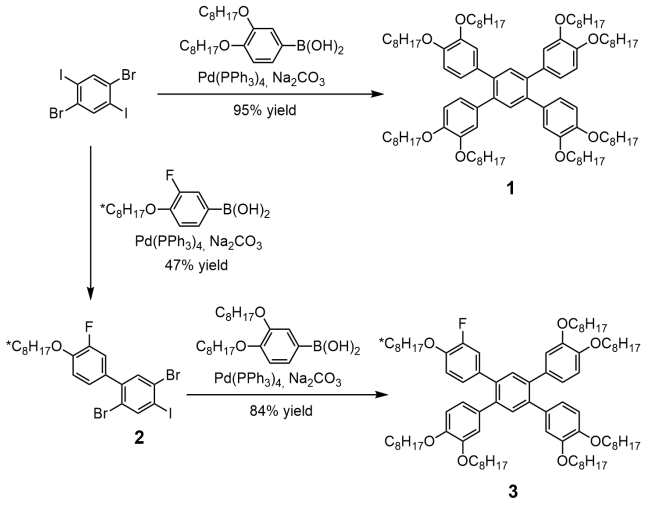

Scheme 1. Synthetic route of discotic liquid crystals.

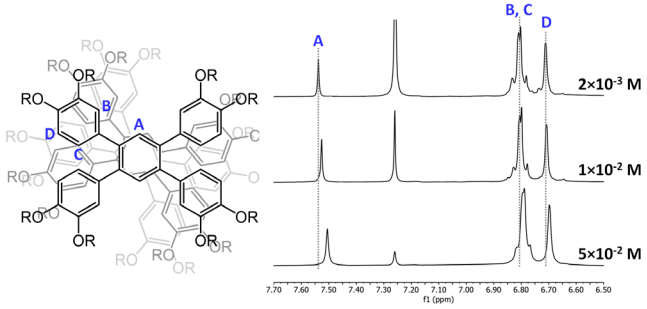

Figure 2. ^{1}H NMR spectra (aromatic region) of **1** in $CDCl_3$ at different concentrations.

The self-assembly of these discotic mesogens was also studied by UV-Vis absorption and fluorescence spectroscopy. Relevant data is presented in **Table 1**. The absorption spectra of **1**, **(*R*)-3**, and **(*S*)-3** were found to be nearly identical, indicating that the introduction of the fluorobenzene unit has minimal impact on the optical properties. We observe a dominant π-π* band at 280 nm in chloroform solution (10^{-7} M), attributable to molecularly dissolved species (**Figure 3a**). Upon increasing the concentration, this absorption band becomes more intense and red-shifts as a result of aggregation. The fluorescence spectra also displayed significant changes at higher concentrations (**Figure 3b**). For a 10^{-8} M solution, the emission arises exclusively from the non-aggregated monomeric form as indicated by the band at 330 nm. At higher concentrations, a new peak at 395 nm was observed, whereas the monomer emission gradually decreases. The red-shifted new band is assigned to aggregated species. Excitation experiments were also performed to study the nature of the emitting species. The excitation spectra recorded at low concentrations (<10^{-7} M) showed a main peak at 280 nm attributable to molecularly dissolved species, whereas at concentrations >10^{-7} M, significant broadening and red-shifting to 310 nm was observed, indicating that the emission arises predominantly from excitation of the aggregated state (**Figure S7**).

Table 1. Absorption and emission properties of **1** and **3** in chloroform solutions.

	C (M)	λ_{abs} (nm)	ε (M^{-1} cm^{-1})[a]	λ_{em} (nm)	Φ_F[b]
1	10^{-6}	295	39260	396	0.23
	10^{-8}	280	33128	331	0.13
(*S*)-3	10^{-6}	294	38359	395	0.21
	10^{-8}	281	32643	331	0.12
(*R*)-3	10^{-6}	294	38554	395	0.21
	10^{-8}	280	32821	331	0.11

[a] Molar extinction coefficient at λ_{abs}. [b] Fluorescent quantum yields relative to quinine sulfate in H_2SO_4 (1M)

Self-assembly of molecules can result in *H*- or *J*-aggregates: *H*-aggregates show an hypsochromic shift of the absorption maximum with respect to the isolated chromophore and exhibit in most cases low or no fluorescence, whereas *J*-aggregates show a bathochromic shift of both the absorption and emission maxima and no quenching occurs in the aggregated state. In the present study, the red-shift in the absorption and emission spectra at higher concentrations (>10^{-7} M), as well as the increase in the molar extinction coefficient and in the quantum yield of aggregates with respect to monomers are indicative of formation of *J*-type aggregates.[28] To evaluate any preferential chiral disposition of these *J*-aggregates, electronic circular dichroism (CD) measurements were performed. However, no CD response was observed in chloroform solution (**Figure S8**).

The self-assembly of **1** and **3** was additionally examined by solvent-dependent fluorescence spectroscopy at constant concentration (10^{-8} M) (**Figure S9**). **Figure 3c** shows I/I_0 ratio (I= emission intensity measured at different tetrahydrofuran/water mixtures; I_0= emission intensity in pure tetrahydrofuran) for various volume percentages of water in tetrahydrofuran. The latter is good solvent for the discotic mesogens, whereas water is a poor solvent. The fluorescence intensity (I) increased about six-fold for the sample containing an 80% water in comparison with the compound dissolved in tetrahydrofuran (I_0). The increase in the emission intensity upon aggregation, rather than

the emission quenching, is also likely enhanced by an aggregation-induced enhanced emission (AIEE) effect, which is probably as a result of attenuated intramolecular rotations.[29]

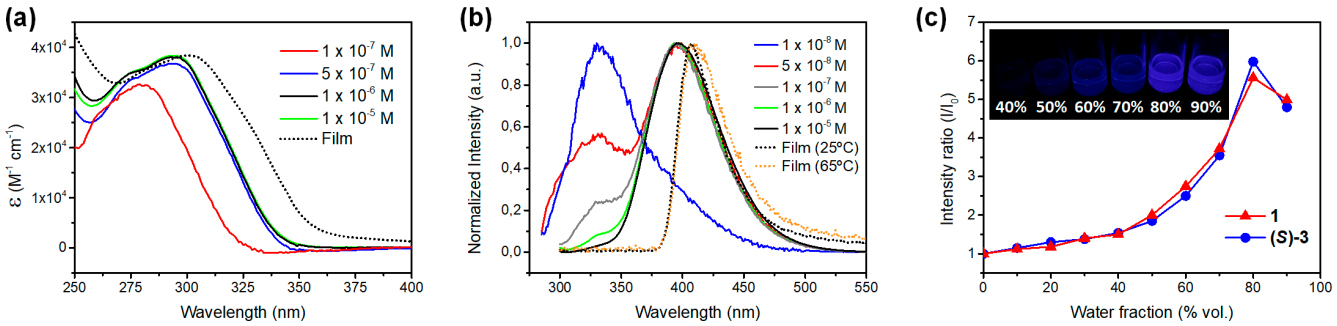

Figure 3. (a) Normalized concentration-dependent absorption spectra of **(*S*)-3** in chloroform solutions and thin film. **(b)** Normalized concentration-dependent changes in emission of **(*S*)-3** in chloroform solutions and thin film. **(c)** Fluorescence intensity ratio (I/I_0) as a function of the percentage of non-solvent for **1** and **(*S*)-3** in tetrahydrofuran/water mixtures (See the Supporting Information for the corresponding emission spectra).

Solid-state fluorescence spectra were recorded at room temperature, wherein **1** and **3** display hexagonal columnar mesophases, and at higher temperatures in the isotropic liquid state (*vide infra*) (**Figure 3b**). The emission bands are red-shifted (*ca.* 10 nm) relative to that in concentrated solutions. These findings confirm intermolecular interactions exist in the mesophase as well as in the isotropic phase, which influence the conformation and hence the electronic delocalization and optical properties.

The thermal stability of **1**, **(*R*)-3**, and **(*S*)-3** were studied by thermogravimetric analysis, and the temperature at which there is 2% weight loss ($T_{2\%}$) was more than >180 °C above their clearing points. Polarized optical microscopy (POM) and differential scanning calorimetry (DSC) were used to study the liquid crystal properties (**Table 2**). Compounds **1**, **(*R*)-3**, and **(*S*)-3** displayed enantiotropic liquid crystal behavior with textures characteristic of hexagonal columnar (Col_h) mesophases (**Figure 4a**). DSC curves were reproducible after the first heating scan, and showed only one peak that corresponds to the clearing point (**Figure 4b**). As deduced from the cooling scan, **1**, **(*R*)-3**, and **(*S*)-3** do not crystallize and retained the mesophase at room temperature. Although no glass transition was found, both compounds were completely rigid at low temperatures and shearing between glass substrates was not possible.

Although the POM textures are characteristic of Col_h mesophases, the absolute assignment of the mesophase was achieved by X-Ray diffraction (XRD). The X-Ray diffraction patterns of the two compounds show the presence of a sharp low-angle peak indicative of the (1 0 0) reflection of the hexagonal lattice (**Figure 4c** and **Figure S10**). Lower intensity (1 1 0) and (2 0 0) peaks provide conclusive proof for the assignment of a hexagonal lattice. These materials also displayed diffuse scattering in the high-angle region (around 4.4 Å). This high angle scattering is from liquid correlations between side chains. Additionally, a second broad reflection at around 4.0 Å was observed, which is indicative of the periodic correlations of the aromatic cores along the columns (parameter *c*). Nonetheless, its weak and broad character rules out the presence of highly ordered Col_h phases with a periodic stacking distance along the columns.

This structural model was additionally evaluated by simple calculations using the measured XRD parameters. The density (ρ) of the compounds in the mesophase can be estimated by the equation $\rho = M \cdot Z/N_A \cdot V$, where M is the molar mass, Z is the number of molecules per disk, N_A is Avogadro's number, and V is the volume of the unit cell ($V = a^2 \cdot \sqrt{3}/2 \cdot c \cdot 10^{-24}$).[30] Considering that each disk is composed by one molecule (Z = 1), reasonable density values (≈ 1.0 g/cm^3) were obtained for all the compounds (**Table 2**). Thus, these calculations support the proposed model for the Col_h phase.

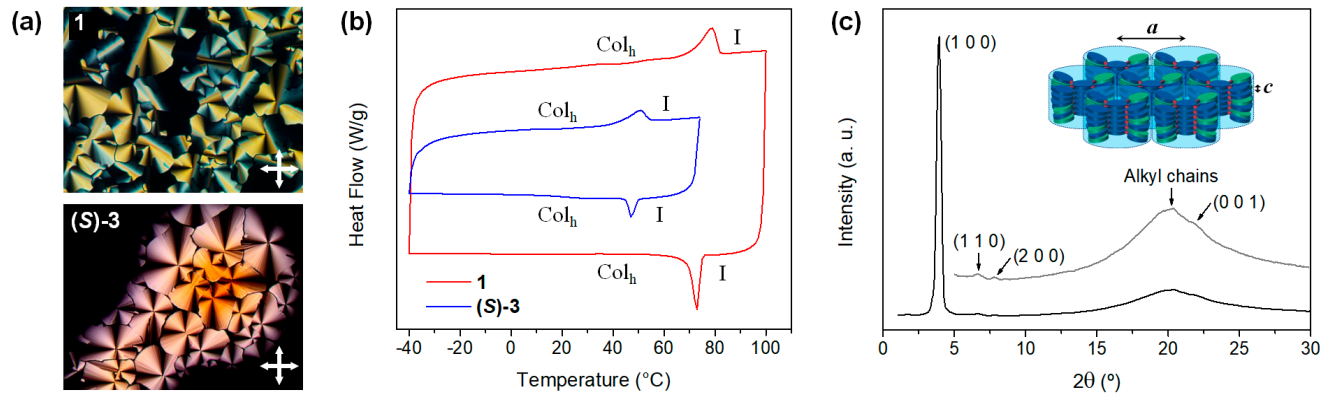

Figure 4. (a) POM microphotographs of the hexagonal columnar mesophase taken at room temperature. **(b)** DSC curves of the second scan (10 °C/min, exo down), and **(c)** 1D XRD profile of **(*S*)-3**.

Table 2. Thermal stability, liquid crystal properties and X-Ray structural parameters.

	$T_{2\%}$ [a] (°C)	Phase Transitions[b]	d_{obs} [c] (Å)	d_{calc} [c] (Å)	$h\ k\ l$ [d]	Lattice parameters[e]
1	263	Col_h 79 (23.9) I	22.5	22.4	1 0 0	a= 25.9 Å; c= 4.0 Å
			12.9	13.0	1 1 0	ρ= 0.99 g/cm^3
			11.2	11.2	2 0 0	
			4.4 (br)		Alkyl chains	
			4.0 (br)		0 0 1	
(*S*)-3	245	Col_h 53 (7.5) I	22.4	22.3	1 0 0	a= 25.8 Å; c= 3.9 Å
			12.8	12.9	1 1 0	ρ= 0.96 g/cm^3
			11.2	11.2	2 0 0	
			4.4 (br)		Alkyl chains	
			3.9 (br)		0 0 1	
(*R*)-3	276	Col_h 55 (6.8) I	22.5	22.3	1 0 0	a= 25.7 Å; c= 3.9 Å
			12.9	12.9	1 1 0	ρ= 0.97 g/cm^3
			11.1	11.1	2 0 0	
			4.4 (br)		Alkyl chains	
			3.9 (br)		0 0 1	

[a] 2% mass loss temperature determined by thermogravimetric analysis.

[b] DSC thermal transitions corresponding to the second heating scan (10 °C/min). Temperatures (°C) are taken from the corresponding peak maximum, and enthalpies (kJ/mol) are shown in brackets. I: isotropic liquid, Col_h: hexagonal columnar mesophase.

[c] d_{obs}: experimental d values obtained from XRD . d_{calc}: calculated d value.

[d] Miller indices.

[e] a: lattice constant of the Col_h phase = $(2/\sqrt{3})\cdot(d_{10}+\sqrt{3}\cdot d_{11}+\sqrt{4}\cdot d_{20}+\ldots)/n_{reflections}$; c: mean stacking distance; ρ: calculated density value.

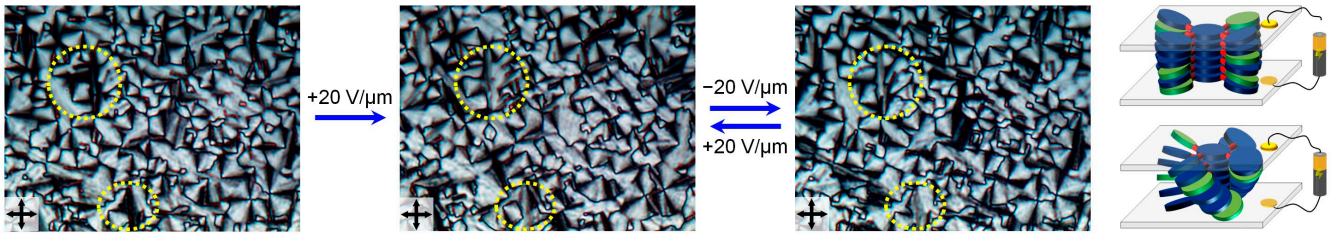

Figure 5. POM images obtained from LC cells of discotic mesogen **(*S*)-3** in the hexagonal columnar phase under zero field or DC electric field (± 20 V/µm), wherein the yellow circles highlight some homeotropic domains in which their birefringence becomes stronger as a response to electric field.

We undertook experiments aimed at inducing chirality in the Col_h phase by applying electric fields. These switching experiments were performed in transparent sandwich-type capacitor cells consisting of two indium tin oxide (ITO)-coated quartz plates separated by 5 µm. The material in the cell was cooled down from the isotropic liquid into the Col_h mesophase at 1 °C/min. Discotic mesogen **1** did not show any electric field response and exhibited a focal conic texture with linear defects, which did not change after the application of a DC electric field of up to 30 V/µm (**Figure S11**).

Cooling down a cell filled with discotic mesogen **(*S*)-3** and **(*R*)-3** through the clearing point at 1 °C/min produces a fan texture with homeotropic domains. When a DC electric field of 20 V/µm is applied, birefringence became stronger. Such birefringence changes can be readily observed in the dark (homeotropic) areas which switch in favor of more birefringent domains (**Figure 5**). The majority of the birefringence changes occur immediately with application of the field and then a slow continuing increase in birefringence takes place and saturates over the 15 min. of electrical field poling. The slower part of the switching process seems to be negligible at low voltages (> 10 V/µm), but is very apparent when the field strength approaches to the electrical break-down of the cells (*ca.* 30 V/µm). These observations suggest that strongly birefringent state is the result of cooperative and net-tilting of the peripheral phenyl rings of discotic **3**, although some minor realignment of the direction of columns cannot be ruled out. The collective directional tilting of the phenyl groups is promoted by biasing of motions by the interaction of the electric field with the lateral dipoles of the fluorobenzene ring. The chiral coupling is also apparent in that positive and negative voltage is applied the material produces two different preferred states (**Figure 5**). These new textures are stable when the field is off and seem stable for several hours, demonstrating that the relaxation process is slow enough.

Electronic circular dichroism (CD) measurements were carried out to evaluate if a preferential chiral assembly is generated in the Col_h phase after applying an external electric field. The initially formed Col_h phase of **(*S*)-3** does not exhibit any neat

CD signal indicative of optical activity. However, a strong positive Cotton effect signal appeared after applying a DC electric field of +20 V/μm at room temperature. The optical activity obtained after applying a negative voltage of -20 V/μm was almost identical to that of obtained with +20 V/μm. Solid-state CD measurements can be affected and distorted by some external factors, such asturbidity, birefringence, or linear dichroism.[31-32] Therefore, we compensate artifacts from the inherent birefringence of liquid crystals by recording and averaging several CD spectra at different cell orientations (rotated and flipped around the light beam), and conclude that this CD response must come from a chiral environment within the Col_h phase. The appearance of a positive Cotton effect at the absorption maximumis consistent with a helical disposition of at least two tetraphenylbenzene chromophores, and this supports a helical stacking model in the columnar arrangement.[33-34] The CD spectra of **(*S*)-3** and **(*R*)-3** present signals of the opposite sign after applying an electric field, indicating enantiomeric helical handedness for both compounds (**Figure S11**). Thus, the preferred helical sense of this Col_h organization is determined by the configuration of the stereogenic center located in the flexible alkyl chain. The fluxional character of **3** allows the system to resolve between two propeller-shaped helical columnar aggregates caused by combination of the chiral side chain and the coupled C-F dipole. The observed chiral resolution results from intercolumnar interactions, as well as the intracolumnar stacking of the propeller-shaped mesogenic cores. Based on this assertion we expect cooperative chiral induction when a small amount of **(*S*)-3** is added to **1**. This fact is observed experimentally, where the electric-field-induced CD signal increases rapidly with the addition of small amounts of **(*S*)-3** to **1** (**Figure S12**). These data confirm cooperative interactions, since a purely unimolecular process would result in a linear relationship between the electric-field-induced CD signal and the mole fraction of **(*S*)-3**.[15]

The observed chiro-optical properties evolve over time, which again reveal the fluxional character of **3** that allows the molecules to progress toward a relaxed non-propeller state correlation along the column after the electric field was turned off, as deduced from the decreased intensity of the CD signals with time (**Figure 6**). However, the electric-field-induced chiral response is apparent after several hours, thereby indicating that the helical supramolecular organization is still present over a time period of at least 24 hours.

To gain more insight into the structure of the assemblies of **3**, we performed theoretical calculations using density functional theory (DFT) and semiempirical methods. A simplified model of **(*S*)-3**, in which the side OC_8H_{17} chains were replaced by shorter OC_4H_9 chains, was used in DFT calculations to reduce the number of atoms (**Figure 7a**). The flexibility of the four phenyl-phenyl bonds of **3** makes possible several minimum-energy structures (**Figure S13**), in which the peripheral phenyl groups rotate out of the plane of the central phenyl ring. The four possible conformers of **3** with ortho phenyl groups orienting oppositely were optimized at the B3LYP-D3/6-31G(d) level. The energies of these conformers are quite similar in energy (within 0.37 kcal/mol), and conformer **(*S*)-3-1** is the most stable. The **(*S*)-3-1** conformer has a nonplanar geometry to minimize the steric hindrance between adjacent phenyl units (**Figure 7b**). The dihedral angle between peripheral and central phenyl groups of **(*S*)-3-1** is around 50°.

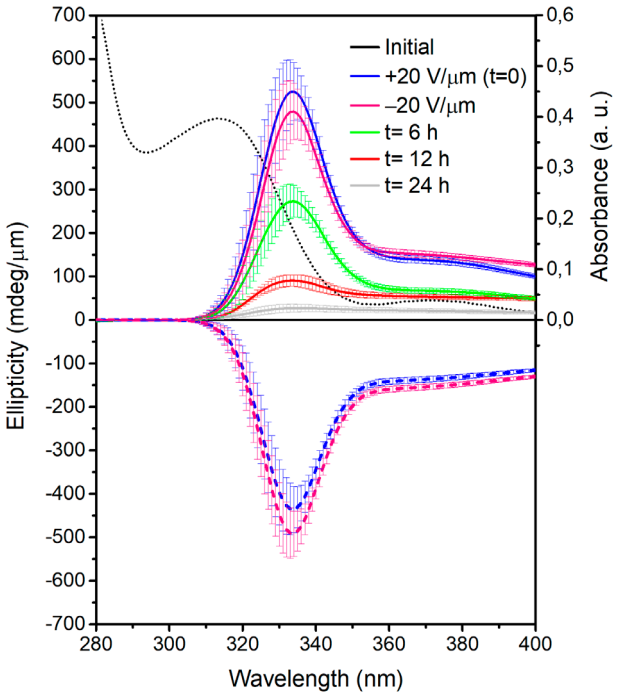

Figure 6. Circular dichroism spectra of **(*S*)-3** (solid lines) and **(*R*)-3** (dashed lines) at room temperature recorded from LC cells under zero field, after applying a DC electric field (± 20 V/μm), and its evolution over time. Error bars were calculated by averaging several CD spectra which were recorded at different orientations measured by rotating (in-plane) and flipping the sample around the light beam. The UV-Vis spectrum of the same sample is shown in dotted black line.

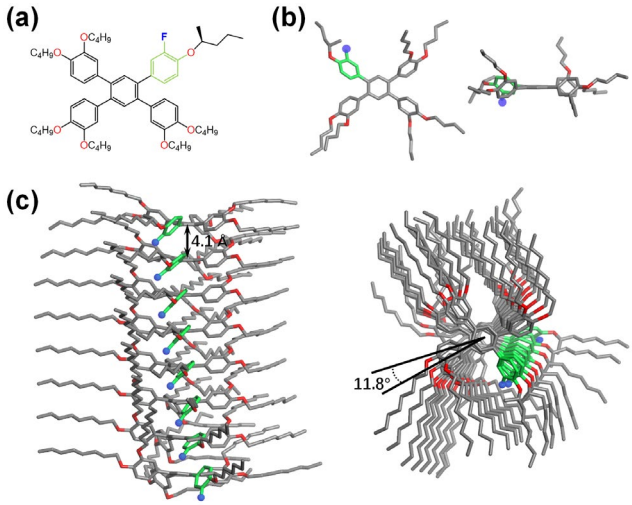

Figure 7. (a) Chemical representation and color scheme of **(*S*)-3** used in the calculations. **(b)** Top and side views of the B3LYP-D3/6-31G(d)-optimized structure calculated for **(*S*)-3-1**. **(c)** Top and side view of the octameric **(*S*)-3** columnar helical stacks calculated using the PM7 semiempirical method (hydrogen atoms have been omitted for clarity).

Based on the molecular geometries obtained by DFT calculations, octameric aggregates were calculated using the semiempirical PM7 method, which is known to provide a reasonable description of weakly bonded supramolecular aggregates. The large molecular size of the octameric aggregate (1816 atoms) precludes the use of more accurate quantum chemical methods. These calculations show that **3** exhibits a planar central benzene core with the peripheral phenyl units rotated

around 50° to maximize π-π interactions between adjacent molecules. This rotation confers the molecule a propeller-like structure that effectively aggregates into a helical column. In this helical arrangement, adjacent stacked molecules are in average separated by 4.1 Å (distance between central benzene planes) and rotated by 11.8° along the stacking axis (**Figure 7b**).

Collectively the calculations suggest that the formation of stable columnar aggregates of discotic molecule **3** is favored by π–π interactions. The fluxional character of discotic mesogens strongly affects the resolution of columnar liquid crystals into chiral structures.[15] In the present case, the columnar phase formed by fluxional **3** molecules has columns that lack a net helicity, as deduced from CD measurements. The rotational freedom of peripheral phenyl groups probably results in an overall average planar conformation, which could also be described as equal populations of diastereometric propellers that would assemble in an equal population of P and M columns. Nonetheless, application of an external electric field biases a net tilting of the fluorobenzene ring out of the plane, and promotes a collective assembly process with one propeller stereoisomer becoming a major conformation of **3**, thereby resulting in a chiral Col_h phase.

CONCLUSIONS

In conclusion, we have prepared a novel class of tetraphenylbenzene-based discotic molecules that can be switched into a meta-stable helical columnar phase by application of an electric field. Absorption and emission studies provide clear evidence for the formation of *J*-aggregates in solution. The discotic mesogens exhibit enhancement of the emission upon aggregation. In condensed phase, the discotic molecules self-assemble into enantiotropic hexagonal columnar phases over a wide temperature range. The columnar liquid crystal phase can be biased towards a chiral helical supramolecular organization in response to an external electric field. The helical arrangement arises from the electric-field-induced tilt of the polar fluorobenzene units that have a proximate stereochemical center. The induced tilt directs all of peripheral phenyl groups into a propeller conformation with respect to the central benzene ring. The preferred helical sense is obtained from the transfer of molecular chirality and a cooperative supramolecular organization. These results demonstrate a promising route to the creation of next-generation chiral materials with various advanced applications, such as chiro-optical switches, or chiro-magnetic materials.

ASSOCIATED CONTENT

Supporting Information. Materials and Characterization Techniques, Synthesis and Characterization, and Supplementary Figures. This material is available free of charge via the Internet at http://pubs.acs.org.

AUTHOR INFORMATION

Corresponding Author

* Email: tswager@mit.edu (T.M.S)

Notes

The authors declare no competing financial interests.

ACKNOWLEDGMENT

We are grateful for support from an Air Force Office of Scientific Research grant: 17RT0904; FA9550-18-1-0341. We are also grateful for computational resources provided by the Massachusetts Green High-Performance Computing Center (MGHPCC) C3DDB cluster. K.Y. thanks Funai Overseas Scholarship for financial support.

REFERENCES

1. Watson, J. D.; Crick, F. H. C., Molecular Structure of Nucleic Acids: A Structure for Deoxyribose Nucleic Acid. *Nature* **1953,** *171* (4356), 737-738.
2. Pauling, L.; Corey, R. B.; Branson, H. R., The structure of proteins: Two hydrogen-bonded helical configurations of the polypeptide chain. *PNAS* **1951,** *37* (4), 205-211.
3. Lee, C. C.; Grenier, C.; Meijer, E. W.; Schenning, A. P. H. J., Preparation and characterization of helical self-assembled nanofibers. *Chem. Soc. Rev.* **2009,** *38* (3), 671-683.
4. Sun, H. J.; Zhang, S.; Percec, V., From structure to function via complex supramolecular dendrimer systems. *Chem. Soc. Rev.* **2015,** *44* (12), 3900-3923.
5. Yashima, E.; Ousaka, N.; Taura, D.; Shimomura, K.; Ikai, T.; Maeda, K., Supramolecular Helical Systems: Helical Assemblies of Small Molecules, Foldamers, and Polymers with Chiral Amplification and Their Functions. *Chem. Rev.* **2016,** *116* (22), 13752-13990.
6. Hwang, M.; Yeom, B., Fabrication of Chiral Materials in Nano- and Microscale. *Chem. Mater.* **2021,** *33* (3), 807-817.
7. *Chirality at the Nanoscale: Nanoparticles, Surfaces, Materials and more*. Amabilino, D. B., Ed. Wiley-VCH Verlag GmbH & Co. KGaA: Weinheim, 2009.
8. Palmans, A. R. A.; Meijer, E. W., Amplification of Chirality in Dynamic Supramolecular Aggregates. *Angew. Chem. Int. Ed.* **2007,** *46* (47), 8948-8968.
9. Rosen, B. M.; Wilson, C. J.; Wilson, D. A.; Peterca, M.; Imam, M. R.; Percec, V., Dendron-Mediated Self-Assembly, Disassembly, and Self-Organization of Complex Systems. *Chem. Rev.* **2009,** *109* (11), 6275-6540.
10. Percec, V.; Glodde, M.; Bera, T. K.; Miura, Y.; Shiyanovskaya, I.; Singer, K. D.; Balagurusamy, V. S. K.; Heiney, P. A.; Schnell, I.; Rapp, A.; Spiess, H. W.; Hudson, S. D.; Duan, H., Self-organization of supramolecular helical dendrimers into complex electronic materials. *Nature* **2002,** *417* (6905), 384-387.
11. Tschierske, C., Nanoscale Stereochemistry in Liquid Crystals. In *Chirality at the Nanoscale*, Amabilino, D. B., Ed. Wiley-VCH Verlag GmbH & Co. KGaA: Weinheim, 2009; pp 271-304.
12. Wang, L.; Urbas, A. M.; Li, Q., Nature-Inspired Emerging Chiral Liquid Crystal Nanostructures: From Molecular Self-Assembly to DNA Mesophase and Nanocolloids. *Adv. Mater.* **2020,** *32* (41), 1801335.
13. Wöhrle, T.; Wurzbach, I.; Kirres, J.; Kostidou, A.; Kapernaum, N.; Litterscheidt, J.; Haenle, J. C.; Staffeld, P.; Baro, A.; Giesselmann, F.; Laschat, S., Discotic Liquid Crystals. *Chem. Rev.* **2016,** *116* (3), 1139-1241.
14. Vera, F.; Serrano, J. L.; Sierra, T., Twists in mesomorphic columnar supramolecular assemblies. *Chem. Soc. Rev.* **2009,** *38* (3), 781-796.
15. Trzaska, S. T.; Hsu, H.-F.; Swager, T. M., Cooperative Chirality in Columnar Liquid Crystals: Studies of Fluxional Octahedral Metallomesogens. *J. Am. Chem. Soc.* **1999,** *121* (18), 4518-4519.
16. Miyajima, D.; Araoka, F.; Takezoe, H.; Kim, J.; Kato, K.; Takata, M.; Aida, T., Ferroelectric Columnar Liquid Crystal Featuring Confined Polar Groups Within Core–Shell Architecture. *Science* **2012,** *336* (6078), 209-213.
17. Miyajima, D.; Araoka, F.; Takezoe, H.; Kim, J.; Kato, K.; Takata, M.; Aida, T., Columnar Liquid Crystal with a Spontaneous Polarization along the Columnar Axis. *J. Am. Chem. Soc.* **2010,** *132* (25), 8530-8531.
18. Yan, X.; Wang, Q.; Chen, X.; Jiang, Y.-B., Supramolecular Chiral Aggregates Exhibiting Nonlinear CD–ee Dependence. *Adv. Mater.* **2020,** *32* (41), 1905667.
19. Zhang, C.; Nakano, K.; Nakamura, M.; Araoka, F.; Tajima, K.; Miyajima, D., Noncentrosymmetric Columnar Liquid Crystals with the Bulk Photovoltaic Effect for Organic Photodetectors. *J. Am. Chem. Soc.* **2020,** *142* (7), 3326-3330.
20. Nguyen, M. L.; Cho, B.-K., Ferroelectrically Switchable Axial Polarization in Columnar Liquid Crystalline Phases. *Chem. Eur. J.* **2020,** *26* (31), 6964-6975.
21. Wu, J.; Takeda, T.; Hoshino, N.; Akutagawa, T., Ferroelectric low-voltage ON/OFF switching of chiral benzene-1,3,5-tricarboxamide derivative. *J. Mater. Chem. C* **2020,** *8* (30), 10283-10289.
22. Hird, M., Fluorinated liquid crystals – properties and applications. *Chem. Soc. Rev.* **2007,** *36* (12), 2070-2095.
23. Madhusudana, N. V., Role of Molecular Dipoles in Liquid Crystals. *Mol. Cryst. Liq. Cryst.* **2004,** *409* (1), 371-387.

24. Zhang, Q.; Peng, H.; Zhang, G.; Lu, Q.; Chang, J.; Dong, Y.; Shi, X.; Wei, J., Facile Bottom-Up Synthesis of Coronene-based 3-Fold Symmetrical and Highly Substituted Nanographenes from Simple Aromatics. *J. Am. Chem. Soc.* **2014,** *136* (13), 5057-5064.
25. Chen, Y.-H.; Liu, S.-F.; Li, H.-A.; Fuh, S.-M.; Lin, H.-C.; Chen, H.-M.; Yang, P.-J.; Chien, S.-C. Photo-crosslinkable liquid crystal monomers with optical activity. *US Pat. Appl. Publ.* 20120289731, **2012**.
26. Benito-Hernández, A.; Pandey, U. K.; Cavero, E.; Termine, R.; García-Frutos, E. M.; Serrano, J. L.; Golemme, A.; Gómez-Lor, B., High Hole Mobility in Triindole-Based Columnar phases: Removing the Bottleneck of Homogeneous Macroscopic Orientation. *Chem. Mater.* **2013,** *25* (2), 117-121.
27. Metzroth, T.; Hoffmann, A.; Martín-Rapún, R.; Smulders, M. M. J.; Pieterse, K.; Palmans, A. R. A.; Vekemans, J. A. J. M.; Meijer, E. W.; Spiess, H. W.; Gauss, J., Unravelling the fine structure of stacked bipyridine diamine-derived C3-discotics as determined by X-ray diffraction, quantum-chemical calculations, Fast-MAS NMR and CD spectroscopy. *Chem. Sci.* **2011,** *2* (1), 69-76.
28. Würthner, F.; Kaiser, T. E.; Saha-Möller, C. R., J-Aggregates: From Serendipitous Discovery to Supramolecular Engineering of Functional Dye Materials. *Angew. Chem. Int. Ed.* **2011,** *50* (15), 3376-3410.
29. Mei, J.; Leung, N. L. C.; Kwok, R. T. K.; Lam, J. W. Y.; Tang, B. Z., Aggregation-Induced Emission: Together We Shine, United We Soar! *Chem. Rev.* **2015,** *115* (21), 11718-11940.
30. Li, Y.; Concellón, A.; Lin, C.-J.; Romero, N. A.; Lin, S.; Swager, T. M., Thiophene-fused polyaromatics: synthesis, columnar liquid crystal, fluorescence and electrochemical properties. *Chem. Sci.* **2020,** *11* (18), 4695-4701.
31. Gottarelli, G.; Lena, S.; Masiero, S.; Pieraccini, S.; Spada, G. P., The use of circular dichroism spectroscopy for studying the chiral molecular self-assembly: An overview. *Chirality* **2008,** *20* (3-4), 471-485.
32. Spector, M. S.; Prasad, S. K.; Weslowski, B. T.; Kamien, R. D.; Selinger, J. V.; Ratna, B. R.; Shashidhar, R., Chiral twisting of a smectic-A liquid crystal. *Physical Review E* **2000,** *61* (4), 3977-3983.
33. Choi, S.-W.; Ha, N. Y.; Shiromo, K.; Rao, N. V. S.; Paul, M. K.; Toyooka, T.; Nishimura, S.; Wu, J. W.; Park, B.; Takanishi, Y.; Ishikawa, K.; Takezoe, H., Photoinduced circular anisotropy in a photochromic W-shaped-molecule-doped polymeric liquid crystal film. *Physical Review E* **2006,** *73* (2), 021702.
34. Vera, F.; Tejedor, R. M.; Romero, P.; Barberá, J.; Ros, M. B.; Serrano, J. L.; Sierra, T., Light-Driven Supramolecular Chirality in Propeller-Like Hydrogen-Bonded Complexes That Show Columnar Mesomorphism. *Angew. Chem. Int. Ed.* **2007,** *46* (11), 1873-1877.

Insert Table of Contents artwork here